# Effects of global climate mitigation on regional air quality and health

- 2 Xinyuan Huang<sup>1</sup>, Vivek Srikrishnan<sup>2</sup>, Jonathan Lamontagne<sup>3</sup>, Klaus Keller<sup>4</sup>, Wei Peng<sup>1,5\*</sup>

- <sup>4</sup> Department of Civil and Environmental Engineering, The Pennsylvania State University,
- 5 University Park, PA, USA.
- 6 <sup>2</sup> Department of Biological and Environmental Engineering, Cornell University, Ithaca, NY, USA.
- <sup>3</sup> Department of Civil and Environmental Engineering, Tufts University, Medford, MA, USA.
- <sup>4</sup> Thayer School of Engineering, Dartmouth College, Hanover, NH, USA.
- <sup>9</sup> School of International Affairs, The Pennsylvania State University, University Park, PA, USA.
- 10 \* Corresponding author: weipeng@psu.edu

Climate mitigation can bring air quality and health co-benefits. How these health impacts might be distributed across countries remains unclear. Here we use a coupled climate-energy-health model to assess the country-varying health effects of a global carbon price across nearly 30,000 future states of the world (SOWs). As a carbon price lowers fossil fuel use, our analysis suggests consistent reductions in ambient fine particulate matter (PM<sub>2.5</sub>) levels and associated mortality risks in countries that currently suffer most from air pollution. For a few less polluted countries, however, a carbon price can increase the mortality risks under some of the considered SOWs, due to emissions increases from bioenergy use and land-use changes. These potential health co-harms are largely driven in our model by the scale and method of deforestation. A robust and quantitative understanding of these distributional outcomes requires improved representations of relevant deep uncertainties, country-specific characteristics, and cross-sector interactions.

Reducing fossil fuel combustion decreases emissions of carbon dioxide as well as toxic air pollutants. As a result, climate mitigation efforts are expected to bring health cobenefits by improving air quality<sup>1</sup>. However, the distribution of these health impacts across countries remains poorly understood. Globally, the pollution and health impacts are already unevenly distributed at present. Half of all deaths attributable to fine particulate matter (technically PM<sub>2.5</sub>) currently occur in China and India<sup>2</sup>, due to high pollution levels combined with the large size of the exposed population. The future health burden in these countries may decrease as air pollution control policies are further tightened to reduced pollution, but may also increase if ageing trends increase the population's vulnerability to air pollution<sup>3,4</sup>.

The air quality and health implications of climate mitigation depend on a range of country-specific characteristics in the energy and social aspects. Reducing fossil fuel combustion often lowers pollution exposure<sup>1,5</sup>, but the magnitude of the air quality co-benefits is affected by the energy mixes. For instance, coal currently accounts for 60% of primary energy use (by EJ) in China, but only 12% in the US<sup>6</sup>, leading to greater health benefits from coal phase-out in China than US<sup>7,8</sup>. In addition, the health effects are influenced by socio-demographic patterns that determine the size and vulnerability of the exposed population. For instance, the elderly population (age 65 or greater, which is more vulnerable to air pollution exposure) is 131 million in China (9.5% of the national total population), as compared to 47 million in the US (15%)<sup>3</sup>. Understanding the differential regional health impacts of climate mitigation thus requires careful consideration of the energy and sociodemographic trends in each region<sup>1,9</sup>.

Another factor complicating the relationship between climate mitigation and reduced mortality is the potential emergence of new sources of air pollution<sup>10</sup>. For example, climate mitigation pathways may involve large-scale production and consumption of bioenergy<sup>11</sup>. This can increase the emissions of PM<sub>2.5</sub> from biomass combustion in end-use sectors<sup>12</sup> and the emissions of ammonia from upstream agricultural activities to produce bioenergy crops<sup>13,14</sup>. Besides the direct emissions from bioenergy production and consumption, bioenergy-heavy futures may also result in increased land competition<sup>15</sup>, leading to

indirect emissions from land use changes (e.g., organic carbon emissions from burning forests<sup>16</sup>). This illustrates the complexities resulting from the multi-sector and multi-regional linkages of the global socioeconomic systems.

How will global climate mitigation affect regional air quality and health in the 21st century? A central challenge in tackling this question is that changes in energy and socioeconomic patterns, which drive future pollution exposure and population vulnerability, are highly complex and uncertain (see Figure 1a for a generic illustration of the complex system dynamics). These uncertainties pose conceptual and methodological difficulties for assessing future air pollution effects and identifying key conditions that result in more or less equitable impact distributions. Here we address this challenge by considering many plausible future states of the world (SOWs) through an exploratory modelling approach<sup>17</sup>. We use a coupled energy-climate-health modelling framework, linking a leading integrated assessment model (Global Change Analysis Model, GCAM<sup>18</sup>) with a reducedform air pollution model<sup>19</sup> and a country-level health impact assessment module<sup>20</sup>, to assess the effects of a global carbon price in nearly 30,000 potential SOWs from 2015 to 2100. We use a carbon price as a proxy for climate mitigation action because it is the most economically efficient way to achieve global decarbonization<sup>21</sup> and has been adopted by many countries and subnational regions to mitigate sectoral or economy-wide emissions<sup>22</sup>.

This study advances the previous literature in three main ways. First, we use an exploratory ensemble approach<sup>23,24</sup> to sample a wide range of socioeconomic and technological uncertainties and to characterize how these uncertainties propagate through a highly interconnected, multisector system to impact air quality and health. We expand on the prior use of a small number of narrative-based scenarios (e.g., the Shared Socioeconomic Pathways<sup>25</sup>) to drastically increase the combinations of uncertain factors being considered. By evaluating a wider range of potential future SOWs, our *a posteriori*, ensemble-based exploratory approach could achieve a clearer picture of the full range of the plausible health outcomes<sup>23,26,27</sup>. It also facilitates the identification of factors (or combinations of factors) which consistently contribute to health co-benefits and co-harms.

Second, we demonstrate possible pathways by which carbon pricing could result in unintended health co-harms under certain SOWs (Figure 1b). Many studies have already demonstrated the direct air quality-related health co-benefits from lowering fossil fuel uses to mitigate climate change<sup>5,28,29</sup>. However, climate mitigation may induce changes in emerging low-carbon technologies and land uses through indirect mechanisms, potentially counteracting the health benefits from lowering fossil fuels. These plausible pathways for health co-harms have not been identified in previous studies which focus on a relatively limited number of scenarios. Our large-scale ensemble approach enables a more careful analysis of potential locations and future conditions where co-harms might occur.

Third, we expand on prior co-benefit studies by focusing on the distributional outcomes across countries. Shifting from aggregate impacts to distributions is crucial to analysing potential inequities and incorporating equity considerations into the global efforts to address climate change, air pollution, and health challenges. Here we focus on the regional distributions of health-relevant metrics, including pollution exposure, mortality risks, and the improvements from carbon pricing. By developing an integrated modelling framework, we trace how a carbon price might drive the future distributional outcomes in health, considering the complex interactions of energy system changes, land use changes, air pollutant emissions, human exposure, and vulnerability.

## Climate change mitigation lowering health risks

We impose an increasing carbon price trajectory on global energy sector CO<sub>2</sub> emissions to approximate a moderate ambition level for climate action: \$28, \$69, and \$117/ton CO<sub>2</sub> in 2030, 2050 and 2100, respectively (Figure 2a). The near-term price level broadly reflects the global policy ambition for the next decade by adding up countries' existing Nationally Determined Contributions<sup>30–32</sup>. The longer-term price level considers only a moderate increase over time and is set at the same magnitude as the highest carbon

price that has been observed so far (i.e., \$103/ton in Sweden and Switzerland, inflationadjusted<sup>22</sup>).

Compared to the SOWs with no carbon price, we estimate that this carbon price trajectory reduces the global average temperature by 0.1°C (based on ensemble median; range 0.1–0.2°C across the considered SOWs) in 2050 and by 0.6°C (range: 0.4–1.1°C) in 2100 (Figure 2b). It suggests that even moderate global mitigation contributes to reduced warming and climate damage. However, with the considered carbon price, the ensemble median end-of-century global mean temperature is estimated to be 2.8°C (range: 2.2–4.3°C; N=14,180) higher than the pre-industrial level (or radiative forcing level at 4.9W/m²; range: 3.6–8.0W/m²). It indicates that achieving 2-degree or stricter climate targets would require more stringent global action beyond current ambitions.

Consistent with prior studies<sup>5,28,29,33</sup>, we find that pricing carbon improves global air quality and reduces average PM<sub>2.5</sub>-attributable death rates. Globally, imposing this carbon price reduces the ensemble median PM<sub>2.5</sub>-attributable death rate by 7% (or 69 deaths per million people; range: 38–108) in 2050 and 11% (or 137 deaths per million people; range: 35–358) in 2100 (Figure 2c). This corresponds to 0.4 (range: 0.2–0.7) million avoided deaths in 2050 and 0.9 (range: 0.2–2.9) million avoided deaths in 2100, or an annual average reduction of 0.5 (range: 0.2–1.1) million deaths from 2015 to 2100. Our findings are broadly consistent with prior studies, though many of them considered more ambitious climate mitigation scenarios and therefore found a larger magnitude of the co-benefits (broad range across studies: 0.8–1.8 million)<sup>5,28,29</sup>. In addition, our assessment of future PM<sub>2.5</sub> concentrations (and the associated health impacts) only consider the changes in precursor air pollutant emissions, but not the effects of changing meteorological conditions under a changing climate.

## Reduced PM<sub>2.5</sub>-related health inequities across regions

Cross-country inequity can be defined and operationalized in different ways. Here we define the distribution of impacts as *equitable* when people in all regions face similar

health outcomes. A policy action, such as pricing carbon, is *equity-improving* when it brings increased benefits to regions that currently suffer worse health outcomes than other regions. The results in the main text focus on one metric for the health outcome, i.e., PM<sub>2.5</sub>-attributable death rates, which measures the health risks. The results for the other health outcomes (e.g., PM<sub>2.5</sub> exposure level and the number of PM<sub>2.5</sub>-attributable deaths) and other equity definitions (e.g., based on country income and age groups) are presented in Supplemental Figures S3-6.To demonstrate how the distributional effects may evolve over time, the main results below are for mid-century (e.g., year 2050); see Supplemental Figures S7-8 for results for more near-term (e.g., year 2030) and longer-term (e.g., year 2100) time periods.

Across all considered SOWs, regional inequities in pollution and health persist throughout the century (Figure 3a). The future PM<sub>2.5</sub>-attributable death rate remains higher in developing countries and emerging economies that are currently exposed to higher levels of air pollution. For example, in the SOWs without a carbon price, India and other South Asian nations have the highest PM<sub>2.5</sub>-attributable death rates in 2050, with an ensemble median exceeding 1,500 deaths per million people. In contrast, the lowest projected death rates occur in Australia, Canada, and Northern Europe, with an ensemble median less than 200 PM<sub>2.5</sub>-attributable deaths per million people.

Pricing carbon reduces, but does not eliminate, the regional inequities (Figure 3b). The health benefits associated with the considered carbon price trajectory are generally greater for regions where the PM<sub>2.5</sub>-attributable death rates are presently high (Figure 2d and Figure 3). For instance, based on the 2050 ensemble median, pricing carbon lowers the PM<sub>2.5</sub>-attributable death rate by 113–293 deaths per million per year (or 9.3–12.5%) in India and other South Asian nations. In comparison, for regions with lower health risk at present, the reduction is only 0.7–0.9 PM<sub>2.5</sub>-attributable deaths per million per year (or 0.2–0.4%) in Australia, the United States, and Northern Europe.

Our results suggest that pricing carbon provides a promising avenue to narrowing current pollution and health inequities. This core insight holds for all considered future time periods (see Supplementary Figures S7–8 for 2030 and 2100 results). It also holds for alternative health outcomes are used such as PM<sub>2.5</sub> exposure level and PM<sub>2.5</sub>-attributable deaths (Supplementary Figures S3–4). In addition, considering other definitions for equity, we find supporting evidence that pricing carbon is likely to improve distributional equity by bringing greater health benefits to lower-income countries and to elderly populations (Supplementary Figures S5–6).

## Competing health pathways from carbon pricing

What causes these differential regional health effects of a global carbon price? Our analysis framework models conceptual pathways through which a carbon price could result in both co-benefits and co-harms (Figure 1a and 1b). *Health co-benefits* can be driven by a reduction in air pollutant emissions from fossil fuel combustion, which is the dominant impact in regions that currently suffer from high pollution and health risks. *Health co-harms* can result from increasing emissions from bioenergy use and land use changes associated with bioenergy production, which is more prominent in the regions with cleaner air at present but may expand bioenergy production in the future. Comparing the SOWs in our ensemble, the relative importance of these two pathways contributes to the regional variations in how a global carbon price affects regional emissions and pollution exposure. We discuss these linkages in turn.

First, imposing the carbon price lowers fossil fuel combustion and increases renewable and bioenergy uses across all world regions (Figure 4a). Yet, the extent of these changes depends on the current energy structures and projected technology costs. For instance, in 2050, the carbon price lowers the share of coal in the primary energy mix by 14 percentage points in India (reducing from 53% to 39% based on ensemble median; range across all SOWs: 11–17 percentage points), but only 5 percentage points in Canada (reducing from 12% to 7% based on ensemble median; range across all SOWs: 3–7 percentage points). This is consistent with the observation that India currently relies more heavily on coal<sup>34</sup>. The carbon price hence leads to a greater reduction in coal use in the model. In comparison, we find the increases in bioenergy shares are comparable across

countries (e.g., increases by 2–5 percentage points across the eight selected world regions, based on the ensemble medians). Here, the small regional variations are largely driven by limited cross-region differences in bioenergy shares in current energy mixes, as well as in future bioenergy supply curves assumed in the model.

How the changes in energy use affect air pollutant emissions depends on which sectors are affected and the stringency of pollution regulation in relevant sectors (Figure 4b). For instance, carbon pricing leads to similar percentage reductions in coal share in Southeast Asia and the United States. Yet, the resulting reduction in per capita sulphur dioxide (SO<sub>2</sub>) emissions is smaller in the US due to more stringent pollution control policies on existing coal facilities<sup>35</sup>.

Several types of precursor emissions collectively influence the concentrations of ambient PM<sub>2.5</sub>. In most countries, the substantial reduction in SO<sub>2</sub> and NO<sub>x</sub> emissions from fossil fuel uses is the dominant factor contributing to lower PM<sub>2.5</sub> concentrations, despite the slight increases in PM<sub>2.5</sub> emissions from the combustion of bioenergy. However, in some countries (e.g., Canada and Russia), we find a substantial increase in organic carbon (OC) emissions during the time frame of 2030–2060 under most of the considered SOWs, leading to a net increase in PM<sub>2.5</sub> concentrations (See Supplementary Figure S21). The elevated OC emissions are an outcome of increased biomass production that intensifies land competition and increases the deforestation of the unmanaged forests (see per capita land use changes in Figure 5a). These co-harms pathway results depend on a range of model assumptions related to bioenergy supply chain, energy-land interactions, and deforestation practices (discussed in the next section).

Finally, regional socio-demographic characteristics affect population vulnerability, influencing health outcomes. For instance, imposing a carbon price results in larger relative increases in Canadian PM<sub>2.5</sub>-attributable death rates than the associated PM<sub>2.5</sub> exposure levels. This is consistent with the combined effect of two factors. First, the nonlinear concentration-response relationships result in greater increases in mortality risks, from one unit increase in PM<sub>2.5</sub> exposure, in locations like Canada where the air is

already relatively clean (see PM<sub>2.5</sub> concentrations without the carbon price in Supplementary Figure S15). Second, the increased population ageing in advanced economies like Canada drives an increase in elderly population that are more vulnerable to pollution exposure (see Supplementary Table S9 for the projected age structures in each region).

## Drivers of potential health co-harms

Health co-harms can arise through changes in bioenergy production and the induced changes in land use and deforestation. To understand key factors and model assumptions that drive the modelled co-harms, we perform a model diagnostic analysis to systematically assess the model behaviours and the realism of key assumptions. Below we summarize the key insights related to the magnitude, location, and timing of the health co-harms. A detailed assessment of all relevant model assumptions is presented in Supplementary Table S3. A simple feasibility check of key technology-related model outcomes is shown in Supplementary Section 5.

First, the deforestation method assumed in the model is a key assumption driving the OC emission increases from deforestation and therefore the magnitude of health co-harms (Figure 5). The model applies historical emission factors for global deforestation based on the Global Fire Emissions Database (GFED)<sup>36</sup>, implicitly assuming most future deforestation would occur through slash-and-burn and thus emit substantial amounts of OC. Yet, other methods of deforestation, such as clearcutting, have become more prevalent and may be the preferred method to convert forests into bio-crop land<sup>37</sup>. We therefore conduct a sensitivity analysis on deforestation method by evaluating an extreme case where all deforestation activities occur through clear-cutting and emit no OC. This assumption would avoid the increase in OC emissions from land use and deforestation, eliminating the health co-harms under all SOWs considered in our ensemble (Figure 5c). This sensitivity analysis identifies that the deforestation method is a key factor in determining the magnitude of the potential health co-harms.

Second, location of the health co-harms is primarily affected by the model assumptions on bioenergy supply chain and energy-land interactions. Imposing a carbon price increases bioenergy use in most world regions. Yet, to meet the rising global demand, where bioenergy production would increase the most depends on two key model assumptions. First, biomass is largely assumed in the model to be globally traded (see more in Supplementary Figure S16). This assumption allows bioenergy to be produced in and exported from countries where it is cheapest to do so. Yet the real-world bioenergy markets are much more fragmented due to a range of logistical and market challenges<sup>38</sup>. Second, the land competition between bioenergy, food, and forest is modelled based on the expected profitability of raising and selling bio-crops relative to other land-use options. Since countries like Canada and Russia are assumed to have large areas of unmanaged forests in the model (Supplementary Figure S17), converting forests to bioenergy land in these countries is more economically attractive compared to other countries (Figure 5a).

Finally, the health co-harms are likely to be a more relevant concern for the first half of the century than the second half. For most countries with potential co-harms, we find the proportion of SOWs with health co-harms gradually increases from now to mid-century, but then slowly disappears towards the end of the century. For example, we observe health co-harms (a higher PM2.5-attributable death rate associated with carbon pricing) in 20% of all SOWs for Canada in 2025 and 15% of all SOWs for Russia in 2035. These proportions increase to 98% and 50% in 2050, then gradually decrease to 5% and <1% in 2100, respectively (see more in Supplementary Figure S22). The increase in the first half of the century is largely a result of increasing bioenergy use and production over time. The decrease in the second half of the century is largely an outcome of reduced land use competition. Especially in the SOWs that assume large agricultural productivity improvements, less cropland is needed to meet food demand in the long-term future, lessoning the land competition between food and bioenergy as well as the scale and emissions impacts from deforestation.

#### Discussion

Our analysis highlights the complexity of the system dynamics through which global climate mitigation can influence the regional distribution of pollution and health effects. While the direct health co-benefits from reducing fossil fuel use are well documented <sup>1,5</sup>, we demonstrate possible ways climate mitigation might increase air pollutant emissions and health risks in some regions <sup>39</sup>. The key pathway for co-harms identified in our study is that carbon pricing can increase PM<sub>2.5</sub> emissions, both from direct bioenergy combustion and, in a handful of countries, also from indirect land use changes such as deforestation. Prior studies have also found intensified land use competition in future mitigation scenarios that rely heavily on bioenergy <sup>15</sup>. While those studies demonstrated emerging risks for food security <sup>40</sup> and water stress <sup>41</sup>, our results suggest that unintended consequences can also occur for air quality and health. It underscores the importance of comprehensive assessment for the sustainability implications of large-scale mitigation responses to climate change.

Examining the pathways for health co-harms are particularly relevant for countries that have reduced their coal dependence and where bioenergy might be pursued as a key decarbonization strategy. Prior studies have shown that the potential for health cobenefits from fossil reduction is often smaller in advanced economies than in the Global South countries due to already stringent pollution standards on existing fossil-based facilities<sup>35,42</sup>. Considering the potential energy-land interactions, our analysis suggests that health co-benefits from fossil reduction will become less prominent as countries advance towards decarbonization, while the potential health co-harms from the mitigation actions will become increasingly important.

Across all considered SOWs, we consistently find greater decreases in PM<sub>2.5</sub>-attributable death rates in countries facing higher health risks, such as China and India. For countries that may experience potential co-harms such as Canada, Russia, and United States, our analysis also identifies possible strategies (e.g., changing deforestation method) that can eliminate the negative health impacts. This demonstrates that pricing carbon can improve global air quality while simultaneously reducing the current health inequity across countries. Such equity-improving outcomes can be expected under a wide range of

plausible futures that vary in socioeconomic trends, energy demand and technology costs, as well as agricultural and land-use patterns.

Our analysis of how pricing carbon could affect health risks samples future uncertainties by considering a large ensemble of future SOWs. However, the links between large-scale climate mitigation, air pollution, and the distribution of associated health impacts are still shrouded in considerable uncertainties not considered in this analysis. Our study does not resolve the effects of a wide range of additional uncertainties relating to model parameterization and structure<sup>43</sup>. For example, assuming that deforestation occurs through clearcutting, rather than burning, effectively eliminates co-harms from our ensemble. Due to the complexity of the coupled multi-region, multi-sector system, our exploratory study takes a crucial initial step towards identifying the model assumptions and combination of uncertainties that might bias the conclusions about the health implications and distributional outcomes. Fruitful avenues for future research include an exploratory ensemble approach combined with scenario discovery methods and additional sensitivity analyses to identify future conditions or development trajectories resulting in a higher likelihood of health co-harms<sup>26,27</sup>. These methods can improve our understanding of failure modes of potential mitigation strategies and help to identify policy portfolios that are more robust to complex dynamics and deep uncertainties.

Our study is still silent on many important questions. For example, how can more refined strategies help to better navigate the complex landscape of climate, economics, and health? A globally uniform carbon price has been used widely in models to represent climate policy, largely due to its simplicity and the appealing theoretical advantage as the most economically efficient way to achieve global decarbonization. However, real-world policies are more diverse and fragmented<sup>44</sup>. Regulations and sector-based measures are widely and typically adopted and nearly everywhere have a bigger impact on emission abatement than directly pricing carbon<sup>45,46</sup>. Representing various types and combinations of policy instruments is particularly important in today's climate policy context, as hundreds of countries now experiment with ways to reach net-zero emissions by midcentury. We hypothesize that these different policy designs would have different

distributional consequences. For instance, compared to a subsidy on rooftop solar systems, electrifying the transport sector may bring greater benefits to populations living near major roads, who are often disproportionately minorities and people of lower socioeconomic status<sup>47</sup>. In addition, the health co-harms identified in our analysis may also be mitigated by imposing land conservation policies along with a carbon price on energy-sector emissions<sup>48</sup>.

A second open question is how much-needed improvements in the representations of health drivers, exposures, and outcomes impact the conclusion. For instance, bioenergy is an important technology driver for the health co-harms observed in our study. Yet, our modelling approach only considers 12 land types for 384 land regions worldwide. A detailed, subnational representation of land-use patterns is essential to identify suitable land for bioenergy production and model the competition between different land-use purposes<sup>49,50</sup>. Assessing the disparities across socio-demographic groups, both for exposure and health outcomes, also requires fine-scale pollution simulation and health impact assessment. While some studies are moving in this direction<sup>51,52</sup>, research that quantifies these linkages at decision-relevant resolutions is still largely in its infancy. These efforts can help in the search for decarbonization strategies that can simultaneously reduce adverse health impacts and associated inequities.

Our study lays the foundation for future efforts to address these open questions and advance our scientific understanding of the coupled energy-land-energy systems. Our work also has important policy implications. We assess the key drivers for the country-varying health effects of climate mitigation and identify potential cross-sector linkages (e.g., between energy and land) that may lead to different distributional impacts. These insights are critically important, both for the international community and individual countries, to incorporate health and equity considerations into their climate mitigation efforts.

#### Methods

#### Construction of state of the world ensemble

We construct a large-scale exploratory ensemble of plausible future states of the world (SOWs) using a leading global-scale, process-based integrated assessment model, GCAM v5.4<sup>18</sup> (Supplementary Table S1). GCAM is a multi-sector model with technology-rich representations of five systems and their interactions: energy, water, agriculture and land use, economy, and climate systems<sup>18</sup>. Based on varying input assumptions on socioeconomic drivers, technology costs, and policy actions, GCAM simulates the behaviours and interactions between these systems and projects future patterns at five-year intervals in a partial equilibrium economic modelling framework. For the GCAM version used in this study (v5.4), the energy and economy sectors are modelled for 32 world regions; the land system is divided into 384 subregions; and the climate/physical Earth system is simulated by a reduced-form climate model, Hector<sup>53</sup>, at the global scale.

For the representation of the decision lever, we consider a simple policy design, i.e., whether a globally uniform carbon price trajectory (Figure 2a) is implemented from 2020–2100. This policy representation reflects the most economically efficient way to reach global decarbonization. Pricing carbon through a tax or a cap-and-trade system has also been widely adopted in many countries and regions to mitigate CO<sub>2</sub> emissions<sup>22</sup>. Our near-term carbon price levels are broadly consistent with the stringency of current carbon markets. We are aware that the real-world climate ambition and carbon price levels vary greatly across regions. For instance, the current carbon prices are \$9.20/ton in China's national emissions trading system (ETS), \$13.89 in the Regional Greenhouse Gas Initiative (RGGI), \$30.82/ton in California, and \$86.53/ton the EU ETS<sup>22</sup>. Meanwhile, most low-income and lower-to-middle-income countries do not have carbon prices<sup>22</sup>. In addition, the recent policy pledges from major economies to reach net-zero emissions by mid-century could substantially strengthen policy stringency in the decades to come. An improved representation of realistic policy choices is therefore an important area for future work<sup>54,55</sup>.

In this study, we sample seven broad categories of future uncertainties in socioeconomic, technological, and land-use aspects (more details in the Supplemental Table S1), including: 1) Population and GDP, since demographics and economic development are fundamental drivers of future human activities, carbon emissions, and health burdens; 2) Price elasticity of energy demand, since the demand for energy influences GHG and air pollutant emissions from end-use and energy supply sectors; 3) Agricultural productivity and income elasticity for food, since food demand and agricultural activities are key determinants for future land use change and related emissions; 4) Fossil fuel extraction costs, since they affect the effectiveness of carbon price in driving down the demand; 5) Low-emissions energy costs, since they affects the competitiveness of low-carbon energy relative to fossil-based technologies; 6) Carbon capture and sequestration (CCS) deployment costs, since they determine the scale of CCS deployment and associated emissions under a carbon price; 7) Water resource availability, since it is a key limiting factor for energy and agricultural activities and therefore affects relevant GHG and air pollutant emissions.

We use a full factorial experimental design across these seven factors to encompass a wide range of plausible futures<sup>23</sup>. Among the seven, the first four (i.e., socioeconomics, energy demand, agricultural and land use, fossil fuel extraction costs) are sampled by considering five sets of assumptions that reflect the storylines of Shared Socioeconomic Pathways (SSPs)<sup>56</sup>. For the other three factors, we sample the future water runoffs using varying levels of groundwater level and reservoir capacity; and we sample the future competitiveness of low-emission energy technologies and cost of CCS technology using varying levels of projected costs. The quantitative assumptions for different SSPs and technology costs are reported in Lamontagne et al. 2018<sup>23</sup> and Calvin et al. 2017<sup>57</sup>.

Combining one decision lever and seven types of uncertainties, we experimented with 30,000 SOWs (i.e., 15,000 pairs with/without a carbon price). However, some SOWs do not yield feasible solutions. For example, the socioeconomic assumption following SSP5 (fossil-fuelled development) is not compatible with AGLU assumption following SSP3

(regional rivalry). This is because SSP3 assumptions for AGLU include low agricultural technology development, restricted trade, lack of land use regulations, but low agricultural productivity are formidable obstacles to achieving high-level socioeconomic developments in SSP5. As a result, we have 14,526 model-solved SOWs without a carbon price and 14,180 model-solved SOWs with a carbon price. Between these two groups, we further pair up the SOWs with the same assumptions for other uncertainties and identify 13,936 pairs of SOWs that only differ in the decision lever. The Supplementary Table S2 provides a comprehensive list of the numbers of solved SOWs categorized by the decision lever (carbon price) and each ensemble design factor.

Since GCAM is an open-source model (download: <a href="http://igcri.github.io/gcam-doc/index.html">http://igcri.github.io/gcam-doc/index.html</a>), here we only include a short description of key energy and land use assumptions that are particularly relevant for this study. In GCAM, the global trade of agricultural commodities is modelled using the Armington approach 58, which assumes that products are differentiated by source and consumers treat goods from different countries as imperfect substitutes. The competition between imports and domestic production is governed by a logit sharing function in each regional market. Global trades of fossil fuels and bioenergy are also modelled using the Armington approach. To avoid unrestricted land conversion to bioenergy production, we apply the default GCAM assumption that protects 90% of all non-commercial lands (i.e., non-commercial pasture and forest, grassland and shrubland) in each geographic land unit (GLU)59. Renewable technologies, such as wind, solar, and geothermal, are not traded. The market shares of different fuels/technologies are governed by their relative or absolute cost difference through logit formulations 60,61. The share weight parameters in the logit functions are resource-specific and calibrated using historical data.

#### Projection of GHG emissions

We project future emissions of annual total GHGs for 32 GCAM regions, by technology and fuel choice. We estimate CO<sub>2</sub> emissions from fossil fuel and limestone uses by multiplying GCAM-projected production and consumption activities with the technology-

specific emission factors estimated from the Carbon Dioxide Information Analysis Center (CDIAC, which is a global inventory of historical carbon emissions from 1751 to 2017<sup>62</sup>). CO<sub>2</sub> emissions from land-use and land-cover change are estimated based on the areas of land use change and the carbon intensity of each land use type<sup>63</sup>.

When a carbon price is imposed, higher-carbon technologies become more expensive whereas lower-carbon technologies become more cost-competitive. This cost difference (along with other non-cost related assumptions) determine the relative contribution of these technologies and fuel choices in meeting the demand in each economic sectors such as electricity, transport, industry, residential and agricultural sectors.

We also calculate the emissions of non-CO<sub>2</sub> GHGs, including methane, nitrous oxide, and fluorinated gases by multiplying relevant activities with the emission factors from EPA 2019<sup>64</sup>. When the carbon price is imposed, the changes in non-CO<sub>2</sub> greenhouse gas emissions are proportional to the changes in activity level, except for the reductions in emission intensity that are adjusted based on the exogenously assumed marginal abatement cost curves:

$$E_t = A_t \cdot EF_t \cdot (1 - MAC(Eprice_t)),$$

where t stands for a five-year-period,  $E_t$  is the non-CO<sub>2</sub> GHG emissions,  $A_t$  is the activity level,  $EF_t$  is emissions factor, MAC is the marginal abatement cost curve, and Eprice<sub>t</sub> is the carbon price level. The regional MAC curves consider a wide range of various technologies and are derived based on the EPA 2019 database<sup>64</sup>.

## Assessment of air pollutant emissions

We estimate the emissions of five types of air pollutants, including ammonia (NH<sub>3</sub>), nitrogen oxides (NO<sub>x</sub>), sulphur dioxide (SO<sub>2</sub>), black carbon (BC), and organic carbon (OC), for 32 GCAM regions, by technology and fuel choice. The emissions are calculated by multiplying relevant activities projected by the model with the respective emission factors derived from historical data<sup>18</sup>. To account for the tightening of air pollution control policies over time, the future emission factors are adjusted based on a declining trend with

increasing income<sup>65</sup>. The technology mix is also adjusted over time by assuming a higher penetration rate of less polluting units<sup>57,65</sup>. Both adjustments vary across five SSPs.

519 Specifically. For each pollutant emitted from each activity type:

$$E_t = A_t \cdot EF_t \cdot (1 - EmCtrl(pcGDP_t))$$

where t stands for a five-year period,  $E_t$  is the air pollutant emissions,  $A_t$  is the activity level,  $EF_t$  is activity-specific emission factor. EmCtrl represents the percent reduction in emission factor as a result of emissions control, which is a function of per capita GDP, pcGDP $_t$ :

$$EmCtrl_{t} = 1 - \frac{1}{1 + \frac{(pcGDP_{t} - pcGDP_{t0})}{steepness}}$$

where *steepness* is a technology- and air pollutant species-specific exogenous factor based on empirical evidence that determines the extent to which the changes in per capita GDP affect the stringency of emissions controls.

## Assessment of climate outcomes

We model the climate system using the Hector model<sup>53</sup> which interacts with the other parts of GCAM at every five-year time step. Hector is a reduced-form global climate carbon-cycle model, representing the most essential global-scale Earth system processes. The inputs to Hector are global total GHG emissions aggregated across all GCAM sectors and regions. Then, Hector reports global average radiative forcing and temperature changes.

#### Assessment of ambient PM<sub>2.5</sub> concentrations

To assess the ambient PM<sub>2.5</sub> concentrations from precursor emissions, we use the TM5-FASST model<sup>19</sup>, a reduced-form source-receptor model for 56 world regions. TM5-FASST is derived from TM5-CTM, a full chemical transport model for which the non-linear changes in pollution formation and wind transport is being considered<sup>66</sup>. The performance

of TM5-FASST was evaluated in a prior publication<sup>28</sup> and demonstrates satisfying model capabilities in estimating ambient PM<sub>2.5</sub> concentrations.

To map from GCAM to TM5-FASST regions, we first downscale the emissions for 32 GCAM regions to 178 countries (see Supplementary Table S4 for GCAM sector mapping), by sector and for 5 types of precursor emissions, using the country-to-region ratios based on the Emission Database for Global Atmospheric Research (EDGAR) data<sup>67</sup> (see Supplementary Table S5 for EDGAR sector mapping). We then re-aggregate country-level emissions to the 56 TM5-FASST regions.

For each year and SOW, we estimate the  $PM_{2.5}$  concentrations using the changes relative to 2000, as the base year, assuming linear relationship between emissions and  $PM_{2.5}$  concentrations as well as additivity across all types of emissions and regions. Specifically, the following equation is used:

561 
$$C(y) = C_{base}(y) + \sum_{x}^{n_x} \sum_{i}^{n_i} A_i[x, y] \cdot [E_i(x) - E_{i,base}(x)]$$

where C(y) and  $C_{base}(y)$  are the ambient PM<sub>2.5</sub> concentration in receptor region y in a future year of interest and in 2000, respectively.  $E_i(x)$  and  $E_{i,base}(x)$  are the emissions of the air pollutant type i from a source region x in a future year of interest and in 2000, respectively.  $A_i[x,y]$  is the source-receptor coefficient, capturing how the emissions of precursor air pollutant type i in source region x would influence the ambient PM<sub>2.5</sub> concentrations in receptor region y.  $n_x$  is the total number of source regions whose emissions affect the ambient PM<sub>2.5</sub> concentration in receptor region y, plus two additional sources, shipping, and aviation, that are not tied to a particular location. i is the index for the type of precursor emissions, which include ammonia (NH<sub>3</sub>), nitrogen oxides (NO<sub>x</sub>), sulphur dioxide (SO<sub>2</sub>), black carbon (BC), and particulate organic matter (POM) that are estimated from GCAM.  $n_i$  is the total number of precursors that form ambient PM<sub>2.5</sub>. The unit of the PM<sub>2.5</sub> concentration is  $\mu g/m^3$ , and the units of the emissions are kTonne/year.

Since TM5-FASST model uses the year 2000 as the base year, the values for  $E_{i,base}(x)$  are taken from the Representative Concentration Pathway (RCP) database for the year

2000 at  $1^{\circ} \times 1^{\circ}$  resolution<sup>19</sup>; using 2000 emissions as input,  $C_{base}(y)$  is estimated using a full chemical transport model TM5-CTM<sup>66</sup>, also at a global  $1^{\circ} \times 1^{\circ}$  resolution. The values in the source-receptor matrix A are derived from a series of perturbation runs that increase the precursor emissions by 20%, by precursor type and source region, and assess the implications on PM<sub>2.5</sub> concentrations in each receptor region.

Although the simplicity of the TM5-FASST model enables our assessment of nearly 30,000 SOWs for many years, there are caveats when using this model for assessing future pollution levels. For instance, it does not consider how a changing climate might influence the pollution formation and transport in the future. It also assumes linear relationships between precursor emissions and resulting PM<sub>2.5</sub> concentrations which simplifies the chemical and physical processes in the atmosphere. To evaluate the performance of TM5-FASST for modelling future pollution levels, we compare the projected PM<sub>2.5</sub> concentrations and health risks using TM5-FASST with the results from the Earth System Model Version 4.1 (ESM4), a high-resolution chemistry-carbon-climate model developed by Geophysical Fluid Dynamics Laboratory. The results from the two models are broadly consistent with each other, suggesting that the TM5-FASST model produces reasonable estimates for PM<sub>2.5</sub> concentrations (see more in Supplementary Section 1.4).

#### Assessment of PM<sub>2.5</sub>-attributable deaths

Following the approach in the Global Burden of Disease Study<sup>2</sup>, we consider six diseases that have been found to be associated with long-term exposure to ambient PM<sub>2.5</sub>, namely chronic obstructive pulmonary disease (COPD), diabetes mellitus type II (DB), ischemic heart disease (IHD), lung cancer (LC), lower respiratory infections (LRI), and stroke.

For each of the five-year age group from 0 to 95+ in each of the 178 countries, we calculate the premature deaths attributable to each of the considered six diseases using the following equation:

 $\Delta Mort = y_0 \cdot AF(c) \cdot Pop,$ 

where  $y_0$  is age- and disease-specific the baseline mortality rate; Pop is the size of the exposed population in each age group; AF is the attributable fraction, which changes with varying exposure levels to PM<sub>2.5</sub> concentration (c) in each region.

Below we describe the data source and calculation methods for each parameter. More detailed information about the input data is provided in the Supplementary Table S6.

For population (Pop), we use age-specific population projections from the IIASA SSP database<sup>56</sup>. The population projections are at country level, with five-year intervals from 2010 to 2100, and vary across the five SSPs.

For baseline mortality rates ( $y_0$ ), we use the age-specific baseline mortality rates for each country projected by the International Futures (IFs) model v7.64<sup>68</sup>, which also vary across the five SSPs. The baseline mortality rates from IFs are projected based on the GDP per capita and education attainment level and calibrated using the GBD 2004 data for cardiovascular diseases, diabetes, malignant neoplasms, respiratory diseases, and respiratory infections. We map IF-reported rates onto the six considered diseases: For IHD and stroke, we use the rates for total cardiovascular disease from IF and multiply by the shares of IHD and stroke in total cardiovascular-disease-related deaths; for LC, we use the rates for malignant neoplasms; for COPD, we use the rates for respiratory disease; for LRI, we use the rates for respiratory infections, and for DB, we use the rates for diabetes. To check the validity of this mapping method, we compared the disease-specific baseline mortality rates calculated using our methods with the rates reported by the GBD study and found them to be largely consistent (see Supplementary Table S7 for the comparison).

For attributable fraction (AF), we calculate the attributable fractions for each disease and age group using the following equation:

$$AF(c) = \frac{RR(c)-1}{RR(c)},$$

where c is the annual mean PM<sub>2.5</sub> concentration in each country and RR is the disease-specific relative risk. The annual mean PM<sub>2.5</sub> concentration c is simulated by TM5-FASST for 56 regions. We further assume all countries within the same TM5-FASST region have the same exposure level. The relative risks are obtained from the GBD study 2019<sup>3</sup> and derived from the Integrated Exposure–Response (IER) model<sup>20</sup> for the six types of diseases for the PM<sub>2.5</sub> exposure levels from 0 to 600  $\mu$ g/m<sup>3</sup>. The RRs are age-specific for IHD and stroke (from 25 to 95+ at five-year intervals) and are for all age-groups for the other four diseases.

## Assessment of the distributional and equity implications

We consider different measurements of equitable distribution and equity-improving distribution that vary in two dimensions, the metric of health outcomes and the definition of health equity. Below we include a brief summary, with more details summarized in the Supplementary Table S8.

Regarding the metric of health outcomes, our main results focus on *health risks* measured by the PM<sub>2.5</sub>-attributable death rate. We also consider two alternative metrics: *health exposure* measured by PM<sub>2.5</sub> concentrations (Supplementary Figure S3) and *health burden* measured by PM<sub>2.5</sub>-attributable deaths (Supplementary Figure S4).

Regarding the definition of health equity, our main results focus on regional variations and consider "equity-improving" outcome as regions that currently face higher health risks benefit more from carbon pricing. We further consider two alternative definitions that focus on variations across different country income groups and global age groups. Here "equity-improving" outcome requires lower-income regions or elderly populations, as more vulnerable regions/groups, benefit more from carbon pricing (Supplemental Figures 5 and 6). To operationalize these definitions, for each metric of health outcomes, we perform an ordinary least square (OLS) regression to statistically evaluate whether the targeted regions/groups indeed benefit more from implementing the global carbon price.

669 670 **Data availability Statement** 671 672 The dataset generated during and analysed in the current study is available from a 673 public zenodo repository (https://doi.org/10.5281/zenodo.6975580). All input data are 674 available in the repository. The output of the GCAM ensemble is not available due to 675 limited space, but the required outputs for the analysis and the production of the tables 676 and the figures in this study are available in the repository. 677 678 **Code availability Statement** 679 680 The GCAM model is available for download from https://github.com/JGCRI/gcam-core. 681 Detailed model documentation is available online at http://jgcri.github.io/gcam-682 doc/index.html. The TM5-FASST model is available at http://tm5-fasst.jrc.ec.europa.eu/. 683 Python (v3.6) and R(v3.6) are used for data analysis. The codes we use to process the 684 data, calculate the health impacts, and make the plots are available from a public 685 zenodo repository (https://doi.org/10.5281/zenodo.6975580). 686 687 Acknowledgements 688 689 X.H., V.S., and W.P. acknowledge the support from the National Science Foundation 690 under Grant No. 2125293. We also thank the seed grant support from Penn State 691 Institutes of Energy and the Environment and Institute for Computational and Data 692 Sciences. K.K.'s contribution was supported by Dartmouth College. We thank Erin 693 Mayfield, Lee Lynd, and Skip Wishbone for invaluable inputs. 694 All errors and opinions are those of the authors and not of the funding entities. 695 696 **Author contribution** 

X.H., V.S., K.K. and W.P. designed the study and interpreted the data. V.S. and J.L. constructed the state of the world ensemble. X.H. led the data analysis and produced the figures. All authors co-wrote the manuscript. **Competing Interests Statement** The authors declare no competing interests. **Figures** 

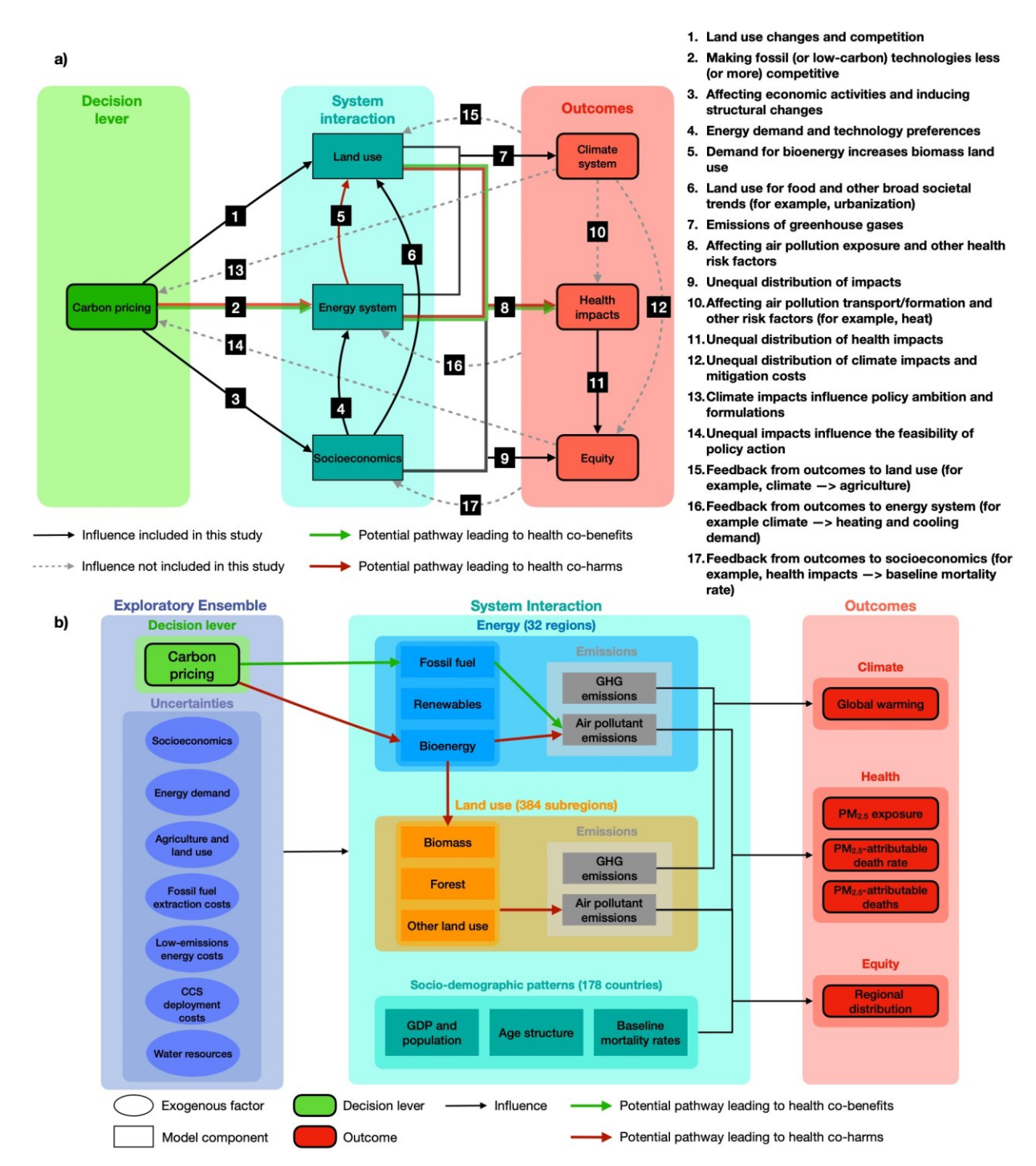
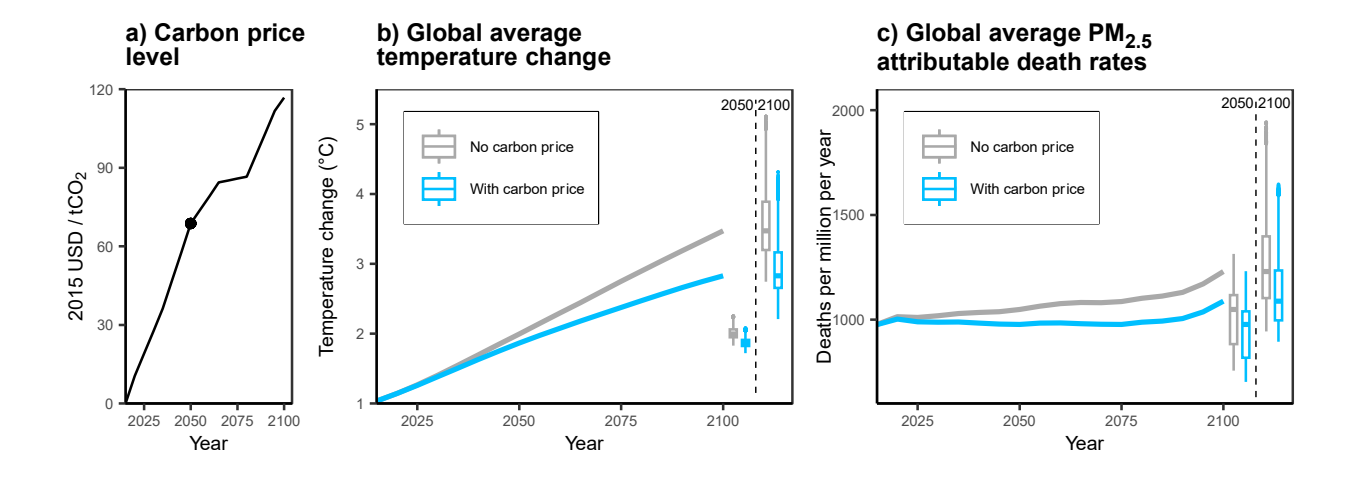


**Figure 1. Pathways for a global carbon price to influence climate, health, and equity outcomes. a:** Conceptual mental model of relevant influences, feedbacks, and system interactions. **b:** Pathways captured by our integrated climate-energy-health model and the uncertainties sampled in our exploratory ensemble. We use the GCAM model to sample future states of the world (SOWs) and implement the carbon price (total ensemble size: N=28,706). We estimate the effects of air pollutant emissions on ambient PM<sub>2.5</sub> concentrations using the TM5-

FASST model<sup>19</sup>. The health impact assessment further uses the projected population and age structure from the IIASA database<sup>56</sup> and the baseline mortality rates from the International Futures model<sup>68</sup>. More details are presented in the Method section.



#### d) Changes in PM<sub>2.5</sub> attributable death rates due to a global carbon price

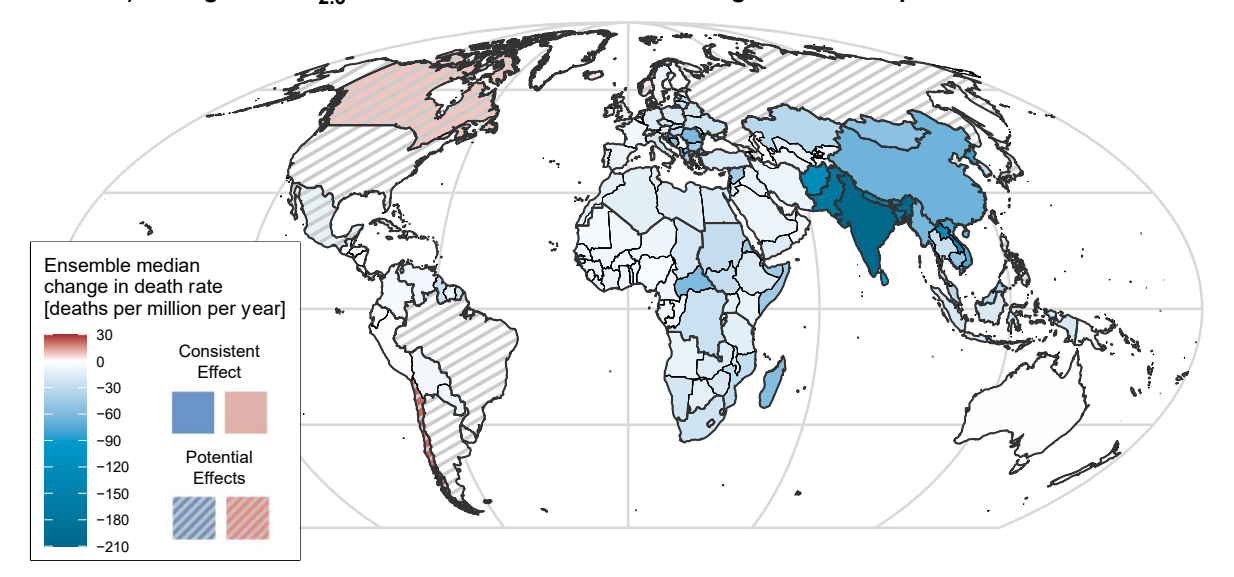


**Figure 2.** Impacts of a global carbon price on future global average temperature and regional distribution of PM<sub>2.5</sub>-attributable death rates. a: The carbon price trajectory from 2015 to 2100 considered in this study; the black dot highlights the price level in 2050 (\$69/ton CO<sub>2</sub>). **b** and **c:** The global average temperature increase relative to the 1850 level and the global annual PM<sub>2.5</sub>-attributable death rates, including the median and ranges of the states of the world (SOWs) with and without a carbon price (N=14,180 and 14,526, respectively; the different sample sizes are because some combinations of input assumptions result in infeasible solutions, more in

Supplementary Information Section 1.2). The borders of the belts are the ranges across all SOWs in each projected year. The box plots on the far right show the ensemble distributions in 2050 and 2100. **d**, Changes in PM<sub>2.5</sub>-attributable death rate in 2050 due to the carbon price (N=13,936; limiting to the pairs of SOWs that have feasible solutions in both cases). "Consistent effects" indicate the same direction of effects (i.e., co-benefits or co-harms) across all the SOWs, whereas "Potential effects" show mixed effects across SOWs. The thicker borderlines show the 32 GCAM regions (except Antarctica) for which the energy/land activities and associated emissions are simulated, whereas the lighter borderlines show 178 regions and countries for which the health impact assessments are performed<sup>69</sup>. See Supplementary Figures S9–S10 for the spatial distribution for 2030 and 2100.



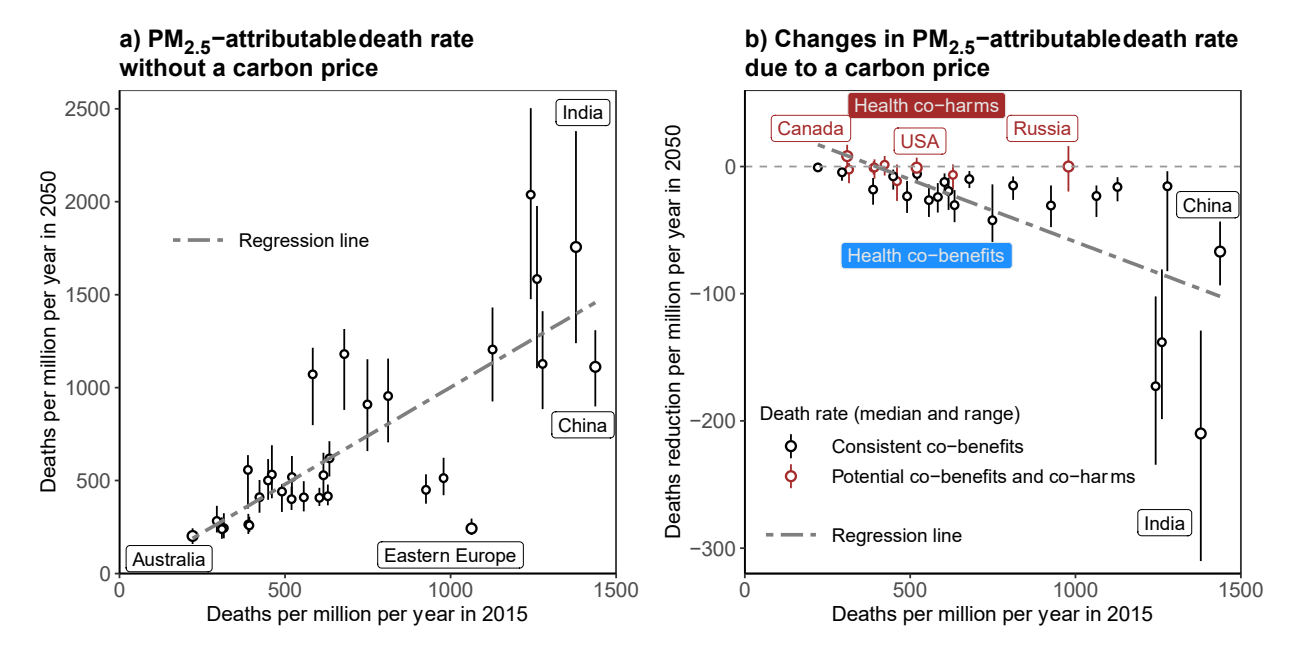


**Figure 3. Distribution of PM**<sub>2.5</sub>**-attributable death rates across regions in 2050. a:** PM<sub>2.5</sub>-attributable death rates without a carbon price. **b:** Changes in the PM<sub>2.5</sub>-attributable death rates as a result of a carbon price. The circles and error bars represent the ensemble medians and ranges for 31 world regions consistent with GCAM regions (excluding Taiwan due to lack of data; N=13,936 for a and b). The grey dashed lines represent the ordinary least square regression line of ensemble medians across regions. In both panels, from left to right, regions are ranked from low to high PM<sub>2.5</sub>-attributable death rates in 2015. See Supplementary Figure S7–8 for the results for 2030 and 2100.

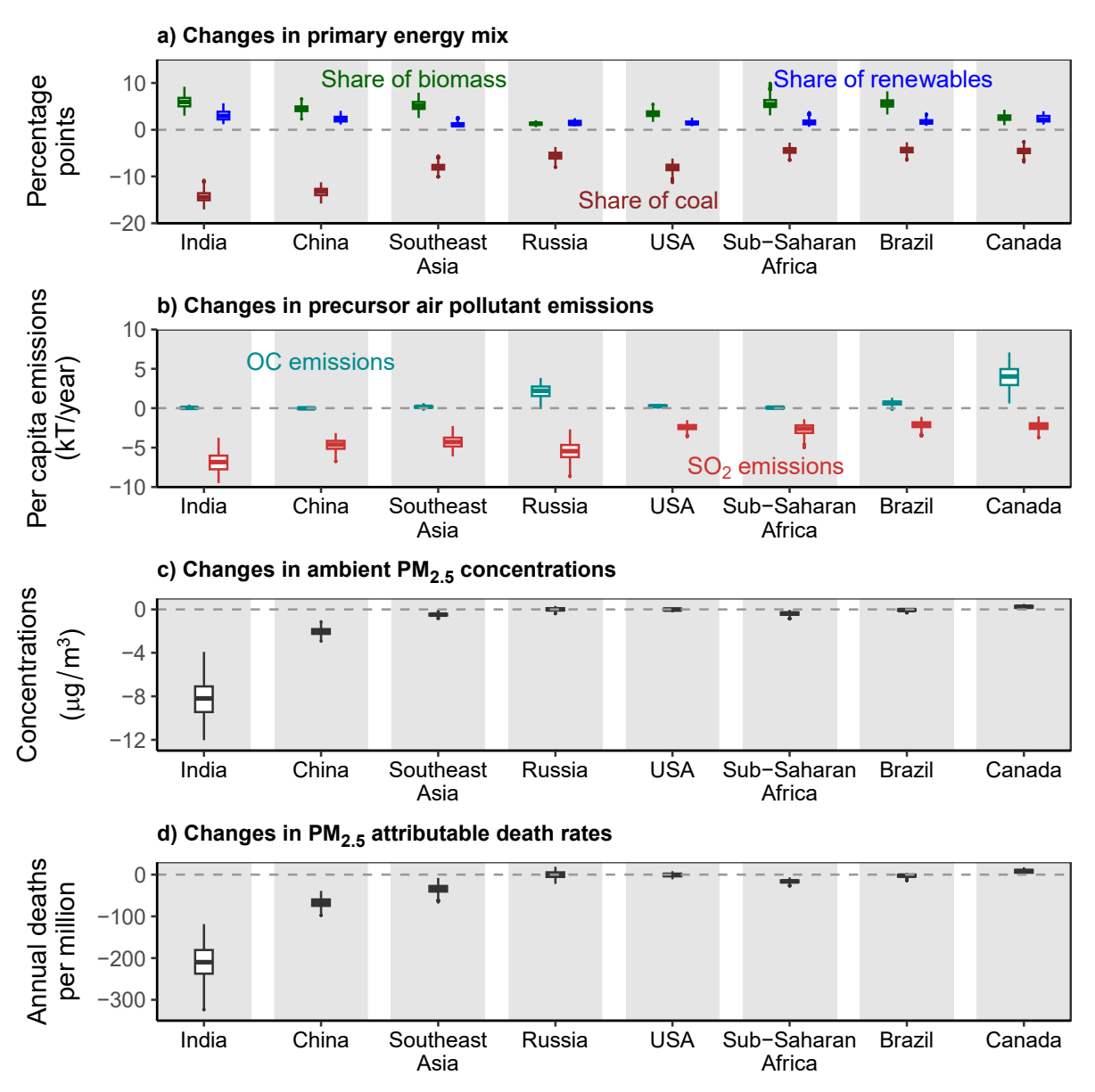


**Figure 4.** Regional changes in the health drivers, exposures, and risks in response to the considered global carbon price in 2050. a: the changes (by percentage points) in shares of coal, biomass, and renewables in the primary energy mix (See Supplementary Figure S18 for global regional-level distributions). b: the changes in organic carbon (OC) and sulphur dioxide (SO<sub>2</sub>) emissions per capita per year (see Supplementary Figure S19 for global regional-level distributions). c: the changes in annual average PM<sub>2.5</sub> concentrations (see Supplementary Figure S20 for global regional-level distributions). d: the changes in PM<sub>2.5</sub>-attributable death rates. The box plots show the ensemble median, quartiles, and range (N=13,936 pairs of states of the world). As representative regions, we include two emerging markets that suffer from the highest pollution and health risks at present (China and India), two lower-income regions that may experience rapid

economic growth and increasing pollution risks in the future (Sub-Saharan Africa and Southeast Asia), two middle-income regions with vast areas of forest resources (Russia and Brazil), and two developed countries with cleaner air and large land areas (the United States and Canada). See Supplementary Figure S11–12 for the results for 2030 and 2100.

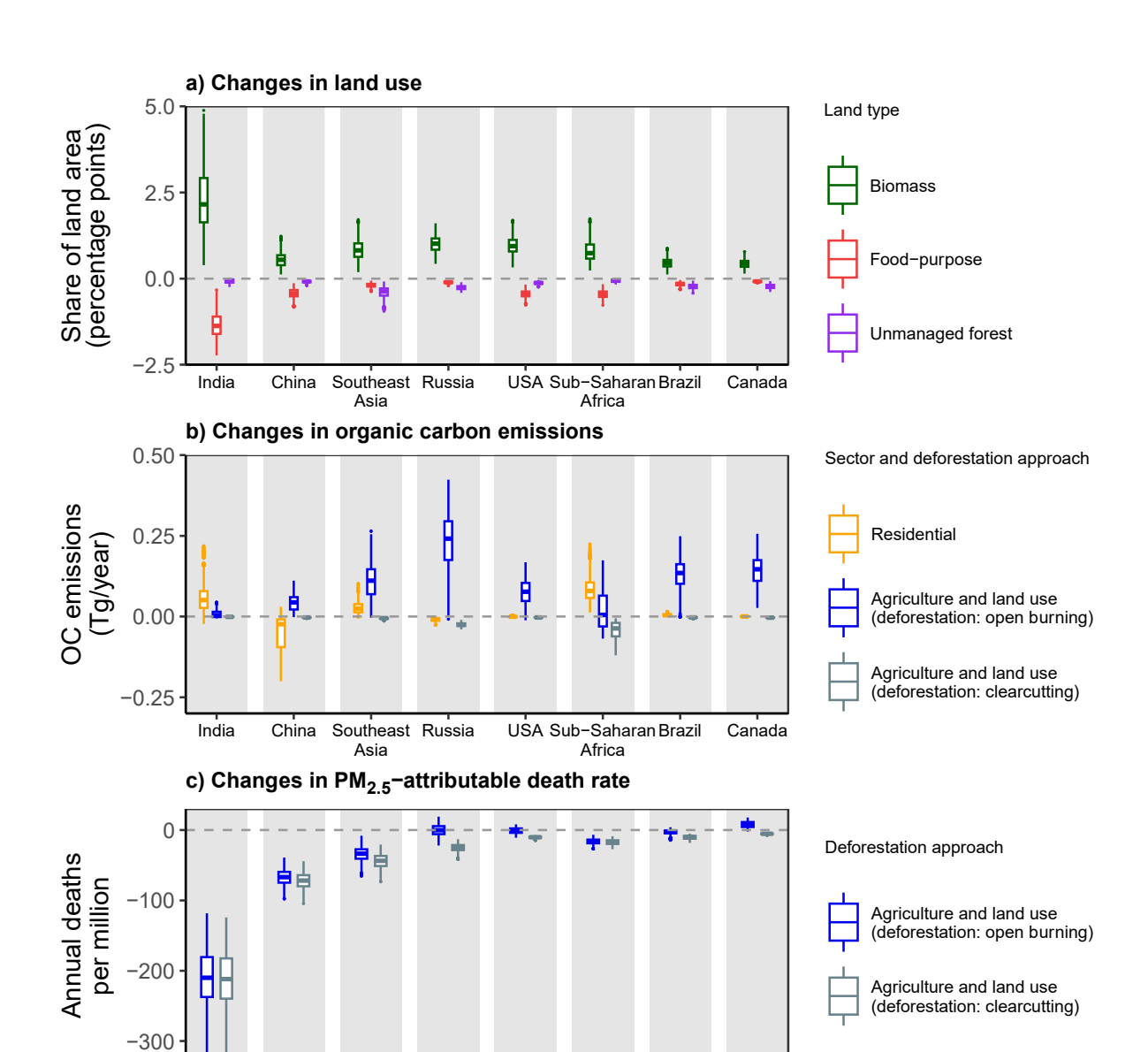


**Figure 5.** Regional changes in land use, organic carbon emissions, and health risks as a result of the considered global carbon price in 2050. a: Changes in land use types (by percentage points). b: Changes in organic carbon emissions in the residential sector and the agriculture and land use sectors. c: Changes in PM<sub>2.5</sub>-attributable death rates. In b and c, we show the sensitivity analysis assuming deforestation occurring through opening burning versus

USA Sub-Saharan Brazil

China

Southeast Russia

clearcutting. The box plots show the ensemble median, quartiles, and range (N=13,936 pairs of states of the world). As representative regions, we include two emerging markets that suffer from the highest pollution and health risks at present (China and India), two lower-income regions that may experience rapid economic growth and increasing pollution risks in the future (Sub-Saharan Africa and Southeast Asia), two middle-income regions with vast areas of forest resources (Russia and Brazil), and two developed countries with cleaner air and large land areas (the United States and Canada). See Supplementary Figure S13–14 for the results for 2030 and 2100.

#### References

779

- 780 1. Driscoll, C. T. *et al.* US power plant carbon standards and clean air and health co-benefits. *Nat. Clim. Change* **5**, 535–540 (2015).
- 782 2. Murray, C. J. L. *et al.* Global burden of 87 risk factors in 204 countries and territories, 1990–2019: a systematic analysis for the Global Burden of Disease Study 2019. *The Lancet* **396**, 1223–1249 (2020).
- 785 3. Yang, H., Huang, X., Westervelt, D., Horowitz, L. & Peng, W. Socio-demographic factors shaping the future global health burden from air pollution. *Nat. Sustain*.
- 4. Shetty, P. Grey matter: ageing in developing countries. *The Lancet* **379**, 1285–1287 (2012).
- West, J. J. *et al.* Co-benefits of mitigating global greenhouse gas emissions for future air quality and human health. *Nat. Clim. Change* **3**, 885–889 (2013).
- 790 6. IEA (2023), 'World energy balances', IEA World Energy Statistics and Balances (database), https://doi.org/10.1787/data-00512-en (accessed on 21 January 2023).
- 792 7. Lelieveld, J. *et al.* Effects of fossil fuel and total anthropogenic emission removal on public health and climate. *Proc. Natl. Acad. Sci.* **116**, 7192–7197 (2019).
- 8. Shindell, D., Faluvegi, G., Seltzer, K. & Shindell, C. Quantified, localized health benefits of accelerated carbon dioxide emissions reductions. *Nat. Clim. Change* **8**, 291–295 (2018).
- Yang, H., Pham, A. T., Landry, J. R., Blumsack, S. A. & Peng, W. Emissions and Health Implications of Pennsylvania's Entry into the Regional Greenhouse Gas Initiative. *Environ.* Sci. Technol. 55, 12153–12161 (2021).
- 10. Owusu, P. A. & Asumadu-Sarkodie, S. A review of renewable energy sources, sustainability issues and climate change mitigation. *Cogent Eng.* **3**, 1167990 (2016).
- 11. Hanssen, S. V. *et al.* The climate change mitigation potential of bioenergy with carbon capture and storage. *Nat. Clim. Change* **10**, 1023–1029 (2020).
- 12. Hill, J. *et al.* Climate change and health costs of air emissions from biofuels and gasoline. *Proc. Natl. Acad. Sci.* **106**, 2077–2082 (2009).
- 13. Masera, O. R., Bailis, R., Drigo, R., Ghilardi, A. & Ruiz-Mercado, I. Environmental Burden of Traditional Bioenergy Use. *Annu. Rev. Environ. Resour.* **40**, 121–150 (2015).
- 807 14. Skorupka, M. & Nosalewicz, A. Ammonia Volatilization from Fertilizer Urea—A New Challenge for Agriculture and Industry in View of Growing Global Demand for Food and Energy Crops. *Agriculture* 11, 822 (2021).
- 15. Popp, A. *et al.* Land-use futures in the shared socio-economic pathways. *Glob. Environ. Change* 42, 331–345 (2017).
- 812 16. Klimont, Z. *et al.* Global anthropogenic emissions of particulate matter including black carbon. *Atmospheric Chem. Phys.* **17**, 8681–8723 (2017).
- 17. Moallemi, E. A., Kwakkel, J., de Haan, F. J. & Bryan, B. A. Exploratory modeling for analyzing coupled human-natural systems under uncertainty. *Glob. Environ. Change* **65**, 102186 (2020).
- 18. Calvin, K. *et al.* GCAM v5.1: representing the linkages between energy, water, land, climate, and economic systems. *Geosci. Model Dev.* **12**, 677–698 (2019).
- 19. Van Dingenen, R. *et al.* TM5-FASST: a global atmospheric source–receptor model for rapid impact analysis of emission changes on air quality and short-lived climate pollutants.
- 821 Atmospheric Chem. Phys. 18, 16173–16211 (2018).

20. Burnett, R. T. *et al.* An Integrated Risk Function for Estimating the Global Burden of Disease Attributable to Ambient Fine Particulate Matter Exposure. *Environ. Health* 

824 *Perspect.* **122**, 397–403 (2014).

- 21. Cramton, P., Ockenfels, A. & Stoft, S. An international carbon-price commitment promotes cooperation. *Econ. Energy Environ. Policy* **4**, 51–64 (2015).
- 22. Carbon pricing dashboard: Up-to-date overview of carbon pricing initiatives. Available at: https://carbonpricingdashboard.worldbank.org/. (Accessed: 15th January 2023).
- 23. Lamontagne, J. R. *et al.* Large Ensemble Analytic Framework for Consequence-Driven Discovery of Climate Change Scenarios. *Earths Future* **6**, 488–504 (2018).
- 24. Dolan, F. *et al.* Modeling the Economic and Environmental Impacts of Land Scarcity Under Deep Uncertainty. *Earths Future* **10**, e2021EF002466 (2022).
- 25. O'Neill, B. C. *et al.* The roads ahead: Narratives for shared socioeconomic pathways describing world futures in the 21st century. *Glob. Environ. Change* **42**, 169–180 (2017).
- 26. Dolan, F. *et al.* Evaluating the economic impact of water scarcity in a changing world. *Nat. Commun.* **12**, 1915 (2021).
- 27. Birnbaum, A., Lamontagne, J., Wild, T., Dolan, F. & Yarlagadda, B. Drivers of Future Physical Water Scarcity and Its Economic Impacts in Latin America and the Caribbean. Earths Future 10, e2022EF002764 (2022).
- 28. Markandya, A. *et al.* Health co-benefits from air pollution and mitigation costs of the Paris Agreement: a modelling study. *Lancet Planet. Health* **2**, e126–e133 (2018).
- 29. Sampedro, J. *et al.* Health co-benefits and mitigation costs as per the Paris Agreement under different technological pathways for energy supply. *Environ. Int.* **136**, 105513 (2020).
- 30. Ou, Y. *et al.* Can updated climate pledges limit warming well below 2°C? *Science* **374**, 693–695 (2021).
- 31. IPCC, 2022: Climate Change 2022: Mitigation of Climate Change. Contribution of Working Group III to the Sixth Assessment Report of the Intergovernmental Panel on Climate Change. Cambridge University Press, Cambridge, UK and New York, NY, USA.
- 32. Fawcett, A. A. *et al.* Can Paris pledges avert severe climate change? *Science* **350**, 1168–1169 (2015).
- 33. Anenberg, S. C. *et al.* Global Air Quality and Health Co-benefits of Mitigating Near-Term Climate Change through Methane and Black Carbon Emission Controls. *Environ. Health Perspect.* **120**, 831–839 (2012).
- 34. IEA. World Energy Outlook 2021, IEA, Paris https://www.iea.org/reports/world-energy-outlook-2021. (2021).
- 35. Lee, J. S. H. *et al.* Toward clearer skies: Challenges in regulating transboundary haze in Southeast Asia. *Environ. Sci. Policy* **55**, 87–95 (2016).
- 36. van der Werf, G. R. *et al.* Global fire emissions and the contribution of deforestation, savanna, forest, agricultural, and peat fires (1997–2009). *Atmospheric Chem. Phys.* **10**, 11707–11735 (2010).
- 37. Pedroso-Junior, Nelson N., Cristina Adams, and Rui SS Murrieta. 'Slash-and-burn agriculture: a system in transformation.' Current trends in human ecology 12.34 (2009): 12-34.
- 38. Proskurina, S., Junginger, M., Heinimö, J., Tekinel, B. & Vakkilainen, E. Global biomass trade for energy—Part 2: Production and trade streams of wood pellets, liquid biofuels,
- charcoal, industrial roundwood and emerging energy biomass. *Biofuels Bioprod. Biorefining* **13**, 371–387 (2019).

- 39. Commane, R. & Schiferl, L. D. Climate mitigation policies for cities must consider air quality impacts. *Chem* **8**, 910–923 (2022).
- 40. Frank, S. *et al.* Reducing greenhouse gas emissions in agriculture without compromising food security? *Environ. Res. Lett.* **12**, 105004 (2017).
- 41. Hejazi, M. I. *et al.* 21st century United States emissions mitigation could increase water stress more than the climate change it is mitigating. *Proc. Natl. Acad. Sci.* **112**, 10635–10640 (2015).
- 42. Wang, K., Yan, M., Wang, Y. & Chang, C.-P. The impact of environmental policy stringency on air quality. *Atmos. Environ.* **231**, 117522 (2020).
- 43. Srikrishnan, V. *et al.* Uncertainty Analysis in Multi-Sector Systems: Considerations for Risk Analysis, Projection, and Planning for Complex Systems. *Earths Future* **10**, e2021EF002644 (2022).
- 44. Weitzman, M. L. Can Negotiating a Uniform Carbon Price Help to Internalize the Global Warming Externality? *J. Assoc. Environ. Resour. Econ.* 1, 29–49 (2014).
- 45. Cullenward, D. & Victor, D. G. Making Climate Policy Work. (John Wiley & Sons, 2020).
- 46. Green, J. F. Does carbon pricing reduce emissions? A review of ex-post analyses. *Environ. Res. Lett.* **16**, 043004 (2021).
- 47. Lee, D.-Y., Elgowainy, A., Kotz, A., Vijayagopal, R. & Marcinkoski, J. Life-cycle implications of hydrogen fuel cell electric vehicle technology for medium- and heavy-duty trucks. *J. Power Sources* **393**, 217–229 (2018).
- 48. Harper, A. B. *et al.* Land-use emissions play a critical role in land-based mitigation for Paris climate targets. *Nat. Commun.* **9**, 2938 (2018).
- 49. Sanchez, D. L., Johnson, N., McCoy, S. T., Turner, P. A. & Mach, K. J. Near-term
   deployment of carbon capture and sequestration from biorefineries in the United States.
   *Proc. Natl. Acad. Sci.* 115, 4875–4880 (2018).
- 50. Kang, Y. *et al.* Bioenergy in China: Evaluation of domestic biomass resources and the associated greenhouse gas mitigation potentials. *Renew. Sustain. Energy Rev.* **127**, 109842 (2020).
- 51. Vohra, K. *et al.* Global mortality from outdoor fine particle pollution generated by fossil fuel combustion: Results from GEOS-Chem. *Environ. Res.* **195**, 110754 (2021).
- 52. Liu, S. *et al.* Spatial-temporal variation characteristics of air pollution in Henan of China: Localized emission inventory, WRF/Chem simulations and potential source contribution analysis. *Sci. Total Environ.* **624**, 396–406 (2018).
- 53. Hartin, C. A., Patel, P., Schwarber, A., Link, R. P. & Bond-Lamberty, B. P. A simple objectoriented and open-source model for scientific and policy analyses of the global climate system – Hector v1.0. *Geosci. Model Dev.* **8**, 939–955 (2015).
- 904 54. Peng, W. *et al.* Climate policy models need to get real about people here's how. *Nature* 905 **594**, 174–176 (2021).
- 55. Stern, P. C., Dietz, T., Nielsen, K. S., Peng, W. & Vandenbergh, M. P. Feasible climate mitigation. *Nat. Clim. Change* **13**, 6–8 (2023).
- 56. Riahi, K. *et al.* The Shared Socioeconomic Pathways and their energy, land use, and greenhouse gas emissions implications: An overview. *Glob. Environ. Change* **42**, 153–168 (2017).
- 911 57. Calvin, K. *et al.* The SSP4: A world of deepening inequality. *Glob. Environ. Change* **42**, 284–296 (2017).

- 913 58. Zhao, X. *et al.* The impact of agricultural trade approaches on global economic modeling. 914 *Glob. Environ. Change* **73**, 102413 (2022).
- 915 59. Plevin, R. J. *et al.* Choices in land representation materially affect modeled biofuel carbon intensity estimates. *J. Clean. Prod.* **349**, 131477 (2022).
- 917 60. Train, K. E. Discrete choice methods with simulation. (Cambridge university press, 2009).
- 918 61. McFadden, D. Conditional logit analysis of qualitative choice behavior. Frontiers in Econometrics (1973).
- 920 62. Environmental Sciences Division, O. R. N. L. Global, Regional, and National Fossil-Fuel CO2 Emissions. (2010) doi:10.3334/CDIAC/00001 V2010.
- 922 63. Kyle, G. P. *et al. GCAM 3.0 Agriculture and Land Use: Data Sources and Methods.* 923 https://www.osti.gov/biblio/1036082 (2011) doi:10.2172/1036082.
- 924 64. Ou, Y. *et al.* Deep mitigation of CO2 and non-CO2 greenhouse gases toward 1.5 °C and 2 °C futures. *Nat. Commun.* **12**, 6245 (2021).
- 926 65. Rao, S. *et al.* Future air pollution in the Shared Socio-economic Pathways. *Glob. Environ.* 927 *Change* **42**, 346–358 (2017).
- 928 66. Krol, M. *et al.* The two-way nested global chemistry-transport zoom model TM5: algorithm and applications. *Atmospheric Chem. Phys.* **5**, 417–432 (2005).
- 930 67. Crippa, M. *et al.* Gridded emissions of air pollutants for the period 1970–2012 within EDGAR v4.3.2. *Earth Syst. Sci. Data* **10**, 1987–2013 (2018).
- 932 68. Hughes, B. B. *et al.* Projections of global health outcomes from 2005 to 2060 using the
  933 International Futures integrated forecasting model. *Bull. World Health Organ.* **89**, 478–486
  934 (2011).
- 69. Original S code by Richard A. Becker and Allan R. Wilks. R version by Ray Brownrigg.
   (2022). mapdata: Extra Map Databases. R package version 2.3.1. https://CRAN.R-project.org/package=mapdata.